Scalable photodetector design with sub-picosecond response time

Ahasan Ahamed[1*], Amita Rawat[1], Lisa N McPhillips[1], Shih-Yuan Wang[2], M Saif Islam[1]

[1]Electrical and Computer Engineering Department, University of California – Davis, California, USA, 95616

[2]W&WSens Devices Inc., 4546 El Camino, Suite 215, Los Altos, California, USA, 94022

ABSTRACT

Addressing the persistent speed-efficiency trade-off, advanced photodetector designs are increasingly incorporating nanophotonic structures to enhance detection efficiency. However, contemporary detector technologies continue to grapple with issues of high-power consumption and limited scalability potential. Embedded nanostructures in photodetectors have already been demonstrated to improve efficiency, gain, and slight improvement in high-speed performance. This paper presents a unique, scalable detector design that leverages nanophotonic enhancement while delivering an ultra-high response time with sub-picosecond full-width-half-maximum for 450 nm illumination wavelength with low breakdown voltage (~8V). Our innovative design strategy involves etching nanoholes into conventional p-i-n photodetectors (1 μm absorbing layer) and doping alternate nanoholes with p+ and n+ doping. The nanoholes are etched all the way through the intrinsic layer to connect with the top and bottom highly doped p+ and n+ doped layer forming a composite vertical-lateral electric field in the photodetector. This technique drastically reduces the effective carrier transport length to mere hundreds of nanometers without diminishing the photon absorption area. As a result, the timing response improves significantly compared to conventional models achieving sharp rise time of ~0.6 ps, fall time of ~8.5 ps, and full width half maximum of <4 ps. Furthermore, the design offers scalability along with advances in lithography processes, setting a promising direction for ultra-high-speed detectors scaling down to <1 ps response time suitable for emerging applications.

Keywords: Ultrafast detectors, Avalanche photodetectors, Sub-picosecond, Nanophotonic structures, CMOS compatible, Scalable.

1. INTRODUCTION

As communication technologies advance, scalable high-speed photodetectors have become crucial for the development and implementation of future generation wireless networks. Ultrafast detectors have a wide range of applications in data communication, Light Detection and Ranging (LiDAR) systems, free space communications, etc[1–5]. Moreover, emerging biomedical research demands picosecond capable photodetectors for higher precision and better resolution imaging using time of flight positron emission tomography (ToF-PET)[6,7]. Ultrafast fluorescence lifetime imaging (FLIM) can reveal complicated biocellular activities by using detectors with sub-picosecond timing resolution[8,9].

Engineering faster photodetectors has always been a challenge for researchers. Several faster materials such as GaAs, CdSe, graphene/$MoTe_2$, and GaN have demonstrated fast response due to their inherent mobility boost[10–13]. However, despite its low mobility, silicon still looks attractive for large-scale production in the industry process[14]. Hsiang et al. showed a 3.7 picosecond timing response using metal-semiconductor-metal (MSM) photodiode designs[14]. Chen et al. used a photoconductive-type detector to report a response time of 1.2 ps[15]. Recently, Heide et al. demonstrated sub-picosecond photon-efficient 3D imaging using single photon avalanche diodes (SPADs)[16].

Increasing the speed of the detector requires them to be thinner such that the RC delay time is reduced. However thinner photodiodes have lower efficiency due to a lack of material to capture photons effectively. This speed-efficiency trade-off

*aahamed@ucdavis.edu; phone 1 530 574-2762

Quantum Sensing and Nano Electronics and Photonics XX, edited by Manijeh Razeghi, Giti A. Khodaparast, Miriam S. Vitiello, Proc. of SPIE Vol. 12895, 128950H
 · 0277-786X · doi: 10.1117/12.3002441

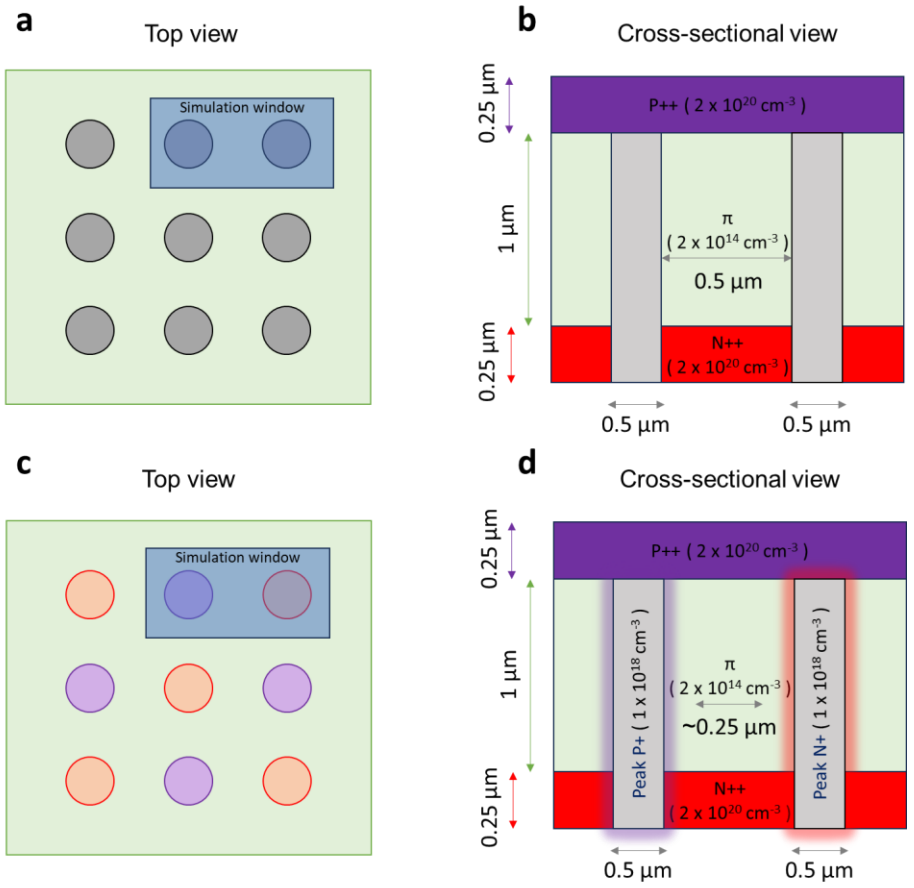

Figure 1: Schematic drawing of the top and cross-sectional view of a photodiode with nanoholes. The top view shows the highlighted simulation window for photodiode with (a) undoped and (c) doped nanoholes. The uniform dopant concentration and dimensions of N++, π, and P++ region is indicated (b) for undoped nanoholes and (d) for doped nanoholes. The nanoholes in (d) are doped with a Gaussian distribution and its peak concentration is shown.

was a bottleneck for silicon photodetectors, which was later resolved using photon-trapping nanostructures[17–20]. These nanoholes can direct the light to propagate laterally allowing it more time to be absorbed efficiently in a thinner region[17,21]. Thus, making them fast sensors capable of 30 ps timing response[22,23]. Furthermore, they can modulate light penetration depth and enhance gain in avalanche photodiodes making them suitable for low-light applications[24–26]. In this paper, we propose a novel photodiode design that utilizes the capabilities of photon-trapping nanoholes and complements it with a better scalable timing response. This is possible by doping the sidewalls of the nanoholes that can modulate the electric fields laterally and transport the carriers through the narrow intrinsic layer width. This achieves a high lateral electric field that lowers the breakdown voltage to 8V from conventional photodiodes 33V. This means that this photodiode can be operated at very low biasing conditions reducing power consumption making them ideal for data center applications. Also, the shorter carrier transit improves the rise time and fall time of the impulse response down to only ~0.6 ps and ~8.5 ps respectively enabling <4 ps full width half maximum for these devices. More importantly, this design can be scaled down by reducing the spacing between nanoholes to further speed up the devices to sub-picosecond capabilities. The photodiode designs can be fabricated using a complementary metal oxide semiconductor (CMOS) compatible fabrication process making them cheaper and easy to implement for a wide range of applications.

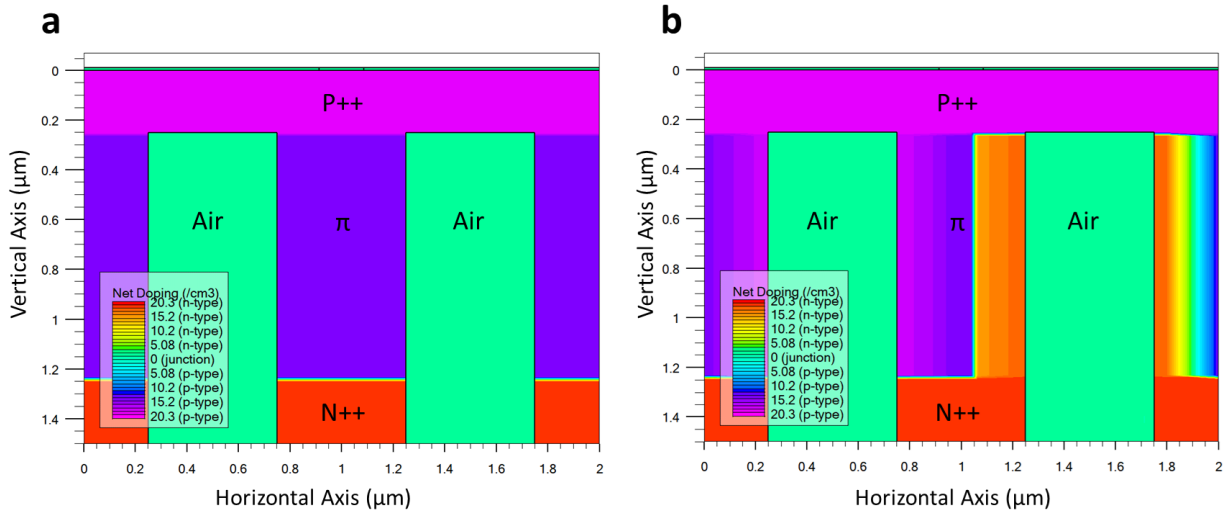

Figure 2: (a) Simulated net doping profile of the PIN photodiode with (a) undoped and (b) doped nanoholes at breakdown condition. Doping the nanoholes reduced the π-layer width to almost 0.25 μm.

2. METHODS AND PROCEDURE

2.1 PIN photodiode design

We use a PIN photodiode structure with 1 μm intrinsic π region sandwiched between two highly doped p++ and n++ regions of 0.25 μm as shown in figure 1. We etch the diode with nanoholes of 0.5 μm diameter each and they are also separated by 0.5 μm from edge to edge. The p++ and n++ layers are doped with 2×10^{20} cm^{-3} impurities while the π layer is doped with 2×10^{14} cm^{-3} p-type impurities. For the photodiode with doped nanoholes, we consider the doping levels inside the nanoholes to be lower than that of the highly doped regions to minimize unintended junctions and electric field spikes. We used a peak dopant concentration of 1×10^{18} cm^{-3} for the nanohole sidewalls that span over 100 nm in both sides shrinking the inner π region width to approximately 0.25 μm.

2.2 Electrical stimulation

We use TCAD software Silvaco ATLAS to simulate the PIN photodiode structures. We used a 2D simulation for simplicity. We first define the regions and doping concentrations in the cross-sectional area shown in Figures 1(b) and 1(d). We have used polysilicon electrodes as neutral contacts for these simulations. For device physics analysis, we considered concentration-dependent mobility and electric field-dependent mobility, Shockley-Read-Hall (SRH) recombination, Auger recombination, optical recombination, and bandgap narrowing as input models for the TCAD simulator. Thereafter we simulated the structure using Newton's numerical method to analyze the electric field, current-voltage relationship, and breakdown voltage of the photodiode structures.

For the high-speed impulse response, we used a sharp optical pulse of 10 fs width. The pulse was generated at 1 ps time originating 0.25 μm away from the bottom center of the photodiode (x = 1 μm, y = 1.75 μm). The peak wavelength of the pulse was 450 nm.

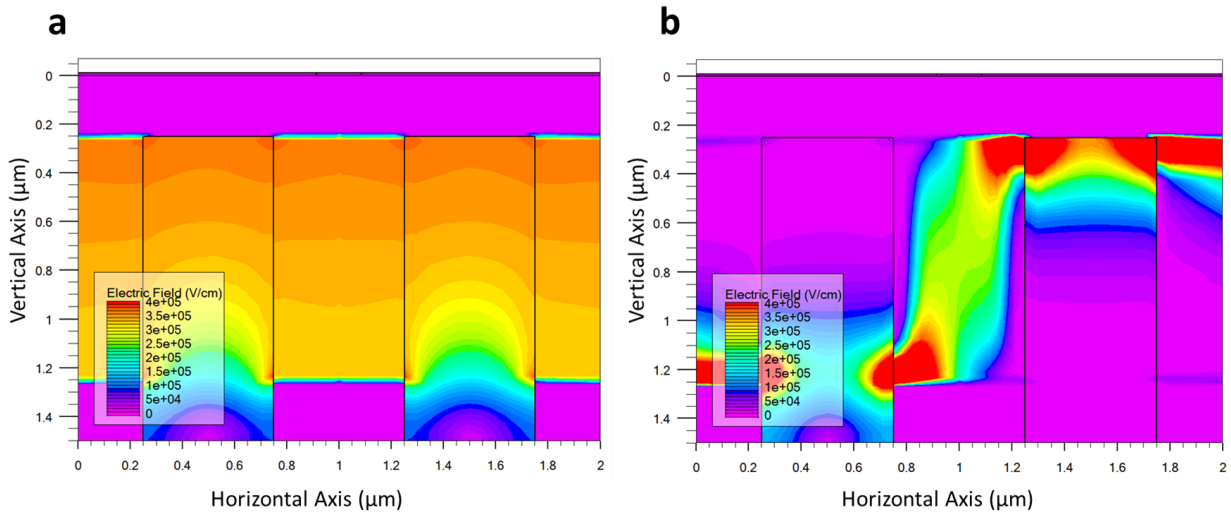

Figure 3: Simulated electric field profile of the PIN photodiode with (a) undoped and (b) doped nanoholes at breakdown condition. The PIN photodiode with undoped nanoholes show only vertical electric field, but in case of the PIN photodiode with doped nanoholes, there is a strong lateral electric field that dominates the carrier transport.

3. RESULTS AND DISCUSSION

3.1 Electric field and breakdown voltage

Upon simulating the structures, we first observe the doping profile shown in Figure 2 to justify our design criteria. Note that the doping concentration is plotted in logarithmic scale as the power of 10, i.e. the maximum doping of 20.3 n-type (red) represents a doping concentration of $10^{20.3}$ cm^{-3} which is equivalent to 2×10^{20} cm^{-3} n-type dopants. For the PIN structure with doped nanoholes in Figure 2(b) we observe that the dopants in the nanoholes do not hamper the net doping of the contact region as they are two orders lower than the contact doping. However, the intrinsic π region has been reduced significantly due to dopant diffusion leaving only hundreds of nanometers. This property was simulated using a Gaussian profile as the diffusion often follows Gaussian distribution.

We show the electric field profiles at near breakdown conditions in Figure 3 for both PIN structures with undoped and doped nanoholes. In the case of the PIN structure with undoped nanoholes in Figure 3(a), the electric field profile is completely vertical with no lateral component. This suggests that the recombined carriers would have to travel the complete thickness of the intrinsic i-layer rendering the photodetector slow in time response. Also, the breakdown voltage would be higher for this case as observed in Figure 4(a). This is because higher voltage is required across a thicker region to generate enough electric field to induce impact ionization. We also simulated a PIN structure without nanoholes and compared its breakdown voltage with a PIN photodiode with undoped nanoholes. As expected, they are quite similar to each other as the electric field profiles in both cases are identical.

On the other hand, the electric field profile in Figure 3(b) shows that the electric field is driven laterally as well as vertically covering almost the whole intrinsic region. This composite field distribution allows us to collect the carries more efficiently. Moreover, the shorter travel distance allows the carriers to be collected much faster than that of conventional structures. This also results in a smaller breakdown voltage which means that even with a low voltage, a strong enough electric field can be generated for impact ionization to occur in this device architecture.

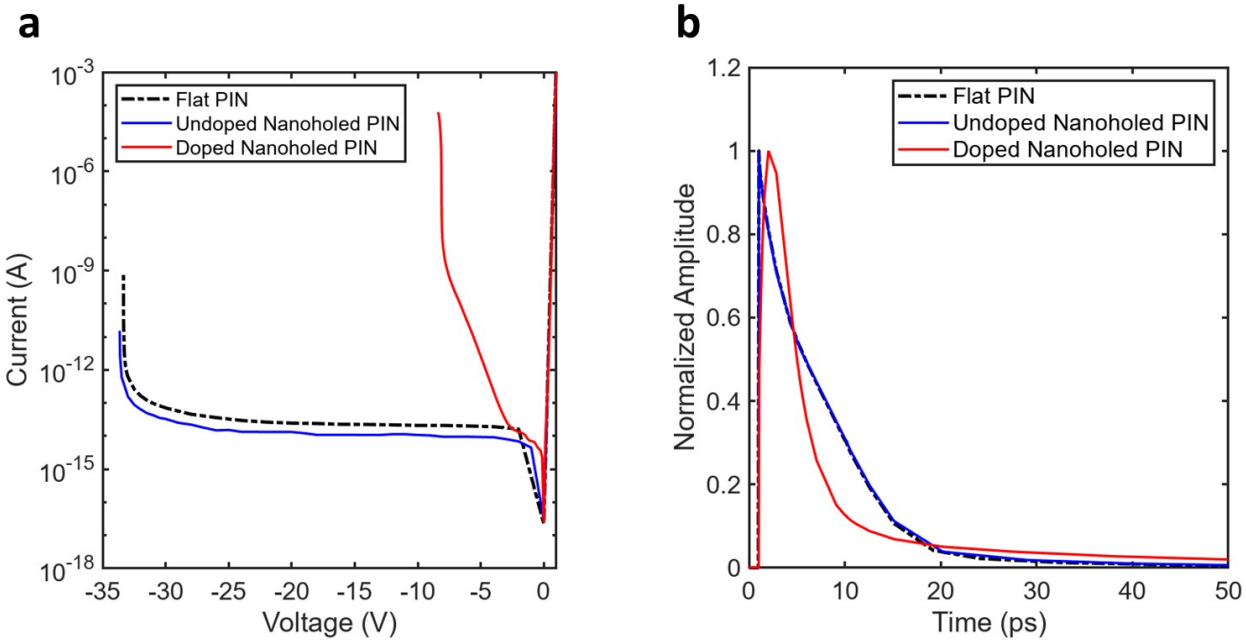

Figure 4: Comparison of the (a) breakdown voltage and (b) transient response among a PIN without nanoholes, PIN with undoped nanoholes, and doped nanoholes. The flat PIN and PIN with undoped nanoholes show similar performance in breakdown voltage and transient response, but PIN with doped nanoholes shows significantly lower breakdown voltage (8V) and a shorter fall time due to the presence of lateral electric fields.

3.2 Transient Response

The transient response characteristics in Figure 4(b) show that the PIN photodiodes without nanoholes (black dashed line) and with undoped nanoholes (blue solid line) show similar performance. This is expected as the electric field profiles governing the carrier transport are identical for both cases. They both have a sharp rise time (~0.02 ps) and longer fall time (~14.5 ps) that contributes to a slow time response as depicted in Table 1. The sharp rise time can be attributed to the small simulation area of the device. Also, the absence of dopant atoms in the intrinsic transport layer provides ballistic transport and no RC delay results in faster response time in the simulation. The long tail is attributed to the longer travel path for carriers as they must travel across the whole intrinsic layer thickness to reach the highly doped contact regions. Therefore, the overall performance is relatively poor giving a full width half maximum of 4.86 ps.

On the other hand, the PIN photodiode with doped nanoholes (red solid line) shows a much better time response with almost half the fall time of ~8.5 ps due to the impact of the lateral field that shortened the traveling distance of the carriers. The rise time increased slightly (~0.6 ps) due to the presence of dopant atoms in the intrinsic region that resists the ballistic transport of photogenerated carriers. Overall, the performance of this novel structure improved the full width half maximum to 3.92 ps. Although this is not a huge improvement, this can easily be scaled down to sub-picosecond by increasing nanohole doping concentration or reducing hole-to-hole distance. Furthermore, for thicker photodiodes with increased efficiency, the timing response would suffer drastically for vertical PIN architecture, while this composite vertical-lateral architecture would provide similar performance as it is determined by the lateral width of the intrinsic π layer rather than vertical thickness. We believe that a complete 3D device simulation would provide a better comparison between the two device designs and providing us with more accurate response time that includes carrier collection efficiency, RC delay and other parasitic contributions.

Table 1: Comparison of breakdown and transient characteristics among different PIN structures

	Flat PIN	**PIN photodiode with undoped nanoholes**	**PIN photodiode with doped nanoholes**
Breakdown voltage	33V	33V	8V
Intrinsic layer thickness	1 μm (vertical)	1 μm (vertical)	~0.25 μm (lateral)
Rise time	0.016 ps	0.0155 ps	0.6198 ps
Fall time	14.1051 ps	14.547 ps	8.5158 ps
FWHM	4.8527 ps	4.8594 ps	3.9157 ps

4. CONCLUSION

Photon-trapping nanoholes are well-known for their efficiency enhancement, reduced capacitance, high speed and gain improvement. This new PIN photodiode design with doped nanoholes will further complement them by manipulating the electric field to our advantage. The lateral electric field reduces the transit time of the carriers and improves the speed of the photodiodes significantly. Enhanced timing response is essential in various applications such as fast data communication, 6G networks, LiDAR communications, biological studies, ultrafast fluorescence lifetime imaging, and more. The ability to scale further adds a technological boost for groundbreaking scientific advancements.

ACKNOWLEDGEMENTS

This work was supported in part by the UC Davis Engineering Dean's Collaborative Research (DECOR) award, the National Institute of Biomedical Imaging and Bioengineering NCIBT grant # 1-P41-EB032840-01, and the National Science Foundation Award Number 2117424 and PFI-TT 2329884.

REFERENCE

[1] Ghandiparsi, S., Devine, E. P., Yamada, T., Wang, S. Y., Islam, M. S., Elrefaie, A. F., Mayet, A. S., Landolsi, T., Bartolo-Perez, C., Cansizoglu, H., Gao, Y., Mamtaz, H. H. and Golgir, H. R., "High-Speed High-Efficiency Photon-Trapping Broadband Silicon PIN Photodiodes for Short-Reach Optical Interconnects in Data Centers," Journal of Lightwave Technology **37**(23), 5748–5755 (2019).

[2] Chi, N., Zhou, Y., Wei, Y. and Hu, F., "Visible Light Communication in 6G: Advances, Challenges, and Prospects," IEEE Vehicular Technology Magazine **15**(4), 93–102 (2020).

[3] Cho, D., Park, J., Kim, T., -, al, Chen, X., Li, D., Zhao, Z., Liu, J., Liu, Y. and Zhu, N., "High-speed photodetectors in optical communication system *," Journal of Semiconductors **38**(12), 121001 (2017).

[4] Royo, S. and Ballesta-Garcia, M., "An Overview of Lidar Imaging Systems for Autonomous Vehicles," Applied Sciences 2019, Vol. 9, Page 4093 **9**(19), 4093 (2019).

[5] Adams, B. W., Elagin, A., Frisch, H. J., Obaid, R., Oberla, E., Vostrikov, A., Wagner, R. G., Wang, J. and Wetstein, M., "Timing characteristics of Large Area Picosecond Photodetectors," Nucl Instrum Methods Phys Res A **795**, 1–11 (2015).

[6] Worstell, W. A., Sajedi, S., Blackberg, L., Feng, Y., Aviles, M. J., Butler, S., Ertley, C. D., Cremer, T., Foley, M. R., Foley, C. J., Hamel, C., Lyashenko, A. V., Minot, M. J., Popecki, M. A., Rivera, T. W., Stochaj, M. E., El Fakhri, G. and Sabet, H., "Measurement of the Parametrized Single-Photon Response Function of a Large Area Picosecond Photodetector for Time-of-Flight PET Applications," IEEE Trans Radiat Plasma Med Sci **5**(5), 651–661 (2021).

[7] Ruckman, L. L. and Varner, G. S., "Sub-10 ps monolithic and low-power photodetector readout," Nucl Instrum Methods Phys Res A **602**(2), 438–445 (2009).

[8] Mokhtari, A., Chesnoy, J. and Chebira, A., "Subpicosecond fluorescence dynamics of dye molecules," JOSA B, Vol. 7, Issue 8, pp. 1551-1557 **7**(8), 1551–1557 (1990).

[9] Margulies, E. A., Wu, Y.-L., Gawel, P., Miller, S. A., Shoer, L. E., Schaller, R. D., Diederich, F. and Wasielewski, M. R., "Sub-Picosecond Singlet Exciton Fission in Cyano-Substituted Diaryltetracenes," Angewandte Chemie **127**(30), 8803–8807 (2015).

[10] Margulis, W. and Sibbett, W., "Picosecond CdSe photodetector," Appl Phys Lett **42**(11), 975–977 (1983).

[11] Li, J., Xu, Y., Hsiang, T. Y. and Donaldson, W. R., "Picosecond response of gallium-nitride metal–semiconductor–metal photodetectors," Appl Phys Lett **84**(12), 2091–2093 (2004).

[12] Zeng, Z., Braun, K., Ge, C., Eberle, M., Zhu, C., Sun, X., Yang, X., Yi, J., Liang, D., Wang, Y., Huang, L., Luo, Z., Li, D., Pan, A. and Wang, X., "Picosecond electrical response in graphene/MoTe2 heterojunction with high responsivity in the near infrared region," Fundamental Research **2**(3), 405–411 (2022).

[13] Chou, S. Y., Liu, M. Y., Fischer, P. B., Hsiang, T. Y., Alexandrou, S. and Sobolewski, R., "Nanoscale sub-picosecond metal-semiconductor-metal photodetectors" (1992).

[14] Hsiang, T. Y., Alexandrou, S., Wang, C.-C., Liu, M. Y. and Chou, S. Y., "Picosecond silicon metal-semiconductor-metal photodiode," https://doi.org/10.1117/12.158589 **2022**, 76–82 (1993).

[15] Chen, Y., Williamson, S. L., Brock, T. and Smith, F. W., "1.9 picosecond optical temporal analyzer using 1.2 picosecond photodetector and gate," Technical Digest - International Electron Devices Meeting, IEDM **1991-January**, 416–421 (1991).

[16] Heide, F., Diamond, S., Lindell, D. B. and Wetzstein, G., "Sub-picosecond photon-efficient 3D imaging using single-photon sensors," Scientific Reports 2018 8:1 **8**(1), 1–8 (2018).

[17] Gao, Y., Cansizoglu, H., Polat, K. G., Ghandiparsi, S., Kaya, A., Mamtaz, H. H., Mayet, A. S., Wang, Y., Zhang, X., Yamada, T., Devine, E. P., Elrefaie, A. F., Wang, S. Y. and Islam, M. S., "Photon-trapping microstructures enable high-speed high-efficiency silicon photodiodes," Nat Photonics (2017).

[18] Kuramochi, E., “Manipulating and trapping light with photonic crystals from fundamental studies to practical applications,” J Mater Chem C Mater **4**(47), 11032–11049 (2016).

[19] Yakimov, A. I., Kirienko, V. V., Bloshkin, A. A., Utkin, D. E. and Dvurechenskii, A. V., “Near-Infrared Photoresponse in Ge/Si Quantum Dots Enhanced by Photon-Trapping Hole Arrays,” Nanomaterials 2021, Vol. 11, Page 2302 **11**(9), 2302 (2021).

[20] Ko, D. H., Tumbleston, J. R., Gadisa, A., Aryal, M., Liu, Y., Lopez, R. and Samulski, E. T., “Light-trapping nano-structures in organic photovoltaic cells,” J Mater Chem **21**(41), 16293–16303 (2011).

[21] Qarony, W., Mayet, A. S., Ponizovskaya-Devine, E., Ghandiparsi, S., Bartolo-Perez, C., Ahamed, A., Rawat, A., Mamtaz, H. H., Yamada, T., Wang, S.-Y. and Islam, M. S., “Achieving higher photoabsorption than group III-V semiconductors in ultrafast thin silicon photodetectors with integrated photon-trapping surface structures,” https://doi.org/10.1117/1.APN.2.5.056001 **2**(5), 056001 (2023).

[22] Bartolo-Perez, C., Qarony, W., Ghandiparsi, S., Mayet, A. S., Ahamed, A., Cansizoglu, H., Gao, Y., Devine, E. P., Yamada, T., Elrefaie, A. F., Wang, S.-Y. and Islam, M. S., “Maximizing Absorption in Photon-Trapping Ultrafast Silicon Photodetectors,” Adv Photonics Res **2**(6), 2000190 (2021).

[23] Yamada, T., Ponizovskaya Devine, E., Ghandiparsi, S., Bartolo-Perez, C., Mayet, A. S., Cansizoglu, H., Gao, Y., Ahamed, A., Wang, S. Y. and Saif Islam, M., “Modeling of nanohole silicon pin/nip photodetectors: Steady state and transient characteristics,” Nanotechnology **32**(36), 365201 (2021).

[24] Bartolo-Perez, C., Chandiparsi, S., Mayet, A. S., Cansizoglu, H., Gao, Y., Qarony, W., AhAmed, A., Wang, S.-Y., Cherry, S. R., Saif Islam, M. and Ariño-Estrada, G., “Avalanche photodetectors with photon trapping structures for biomedical imaging applications,” Opt Express **29**(12), 19024 (2021).

[25] Ahamed, A., Bartolo-Perez, C., Sulaiman Mayet, A., GhandiParsi, S., Zhou, X., Bec, J., Dhar, N. K., Devine, E. P., Wang, S.-Y., Ariño-Estrada, G., Marcu, L., Saif Islam, M., Ahamed, A. and Ghandiparsi, S., “Controlling light penetration depth to amplify the gain in ultra-fast silicon APDs and SPADs using photon-trapping nanostructures,” https://doi.org/10.1117/12.2597835 **11800**(3), 118000F (2021).

[26] Bartolo-Perez, C., Ahamed, A., Mayet, A. S., Rawat, A., McPhillips, L., Ghandiparsi, S., Bec, J., Ariño-Estrada, G., Cherry, S., Wang, S.-Y., Marcu, L. and Islam, M. S., “Engineering the gain and bandwidth in avalanche photodetectors,” Opt Express **30**(10) (2022).

[27] Mayet, A. S., Cansizoglu, H., Gao, Y., Ghandiparsi, S., Kaya, A., Bartolo-Perez, C., AlHalaili, B., Yamada, T., Ponizovskaya Devine, E., Elrefaie, A. F., Wang, S.-Y. and Islam, M. S., “Surface passivation of silicon photonic devices with high surface-to-volume-ratio nanostructures,” Journal of the Optical Society of America B **35**(5), 1059 (2018).

[28] Gao, Y., Cansizoglu, H., Polat, K. G., Ghandiparsi, S., Kaya, A., Mamtaz, H. H., Mayet, A. S., Wang, Y., Zhang, X., Yamada, T., Devine, E. P., Elrefaie, A. F., Wang, S. Y. and Islam, M. S., “Photon-trapping microstructures enable high-speed high-efficiency silicon photodiodes,” Nat Photonics (2017).

[29] Rawat, A., Ahamed, A., Bartolo-Perez, C., Mayet, A. S., McPhillips, L. N. and Islam, M. S., “Design and Fabrication of High-Efficiency, Low-Power, and Low-Leakage Si-Avalanche Photodiodes for Low-Light Sensing,” ACS Photonics **10**(5), 1416–1423 (2023).